Mech. Sci., 16, 921–930, 2025
https://doi.org/10.5194/ms-16-921-2025

Mechanical Sciences
Open Access

Research on dynamic characteristics of motorized spindle based on comprehensive stiffness of angular contact ball bearing

Boqian Dong[1], Chunli Lei[2], Kai Liu[2], Ruizhe Song[2], and Pan Cui[2]

[1]School of Construction Machinery, Chang'an University, Xi'an City, Shaanxi Province 710064, China
[2]School of Mechanical and Electrical Engineering, Lanzhou University of Technology, 36 Pengjiaping Road, Qilihe District, Lanzhou City, Gansu Province 730050, China

Correspondence: Chunli Lei (lclyq2004@163.com)

Received: 27 June 2025 – Revised: 19 September 2025 – Accepted: 8 November 2025 – Published: 2 December 2025

Abstract. In order to study the dynamic performance of a motorized spindle system more accurately and to consider the centrifugal effect, thermal effect of the angular contact ball bearing (ACBB) caused by high speed and influence of temperature rise on the dynamic viscosity of lubricating oil, a comprehensive stiffness model of a motorized spindle support bearing is established. Second, on this basis, combined with the Timoshenko beam theory and rotor dynamics, the dynamic model of the motorized spindle system is proposed using the finite element method. Finally, the influence of various factors on the dynamic characteristics of the high-speed motorized spindle system is studied and verified by experiments. The results show that the increase in the ball bearing preload and axial load could effectively improve the stability of the motorized spindle system, and the increase in the speed and thermal deformation of the ball bearing make the natural frequency and critical speed of the system decrease.

1 Introduction

A high-speed motorized spindle is the key functional component of computer numerical control (CNC) machine tools. This largely determines the high-speed motorized spindle, which is the core component that realizes the high speed and precision of the motorized spindle. Its stiffness in particular directly affects the overall stiffness of the motorized spindle system, which affects the stability and reliability of the system. Therefore, research on the stiffness of the angular contact ball bearing (ACBB) is the primary task when studying the dynamic characteristics of a motorized spindle. In the literature, when calculating the bearing stiffness, most scholars only equate the bearing stiffness to the contact stiffness, while ignoring the film stiffness (Noel et al., 2013; Wang et al., 2024; Li et al., 2020, 2024). Later, it was found that the order of magnitude of film stiffness under lubrication conditions is usually the same as that of contact stiffness, even higher than that of contact stiffness (Chen et al., 2013). Therefore, the contact stiffness and film stiffness should be considered simultaneously when studying the dynamic characteristics of a bearing. Wu (2011) proposed the concept and calculation idea of comprehensive stiffness of a rolling bearing and established an analytical calculation model of the comprehensive stiffness of a rolling bearing that considers lubricating film and the elastic deformation of the inner ring, outer ring and rolling element. However, the thermal effect was not considered. By considering the influence of the thermal effect and high-speed effect on the dynamics of the ACBB during rotation, the research group established the comprehensive stiffness calculation model of ball bearings (Lei et al., 2020, 2021; Li et al., 2020; Liu et al., 2023).

At the same time, scholars both domestic and abroad have some achievements in researching the dynamic characteristics of rotor-bearing systems. Nelson (1980) established the dynamic equation of a rotor system that considers the shear effect using the finite element method. Jorgensen and Shin (1998) built a dynamic model of the spindle-bearing system based on Timoshenko beam theory and carried out numerical calculation, verified by experiments. Fawzi (1998) used

the finite element method to calculate the natural frequency, modal response and dynamic response of the rotor-bearing system, considering translational motion, moment of inertia, shear deformation, gyroscopic moment and system damping. Cao and Yusuf (2004) proposed a general method for calculating the dynamics of the spindle-bearing system based on Timoshenko beam theory. Li (2006) analyzed the internal dynamic state of the bearing, then proposed the dynamic model of the super-high-speed motorized spindle system using the finite element method and studied the factors influencing the dynamic performance of the system. Holkup and Cao (2011) systematically studied the dynamic performance of the spindle under different working conditions and different preloading. Cao et al. (2012) considered the centrifugal force and gyroscopic moment effect of rotating parts and presented the dynamic model of the spindle-bearing system using the finite element method. Fang et al. (2021) proposed a qualitative and quantitative analysis method for the rotor-bearing system supported by angular contact ball bearings. Lin et al. (2003) established a thermo-mechanical dynamic model of a high-speed spindle system and analyzed the influence of centrifugal effect and gyroscopic effect on the dynamic characteristics of the spindle when it rotates at high speed. Zhang and Chen (2016) established the thermal-dynamic models of bearings and rotating shafts, then analyzed the influencing factors. Cheng (2019) considered the influence of various factors on the deformation of the bearing and the spindle, and constructed a dynamic model of the motorized spindle system under the thermal-mechanical coupling condition. It can be seen from the above literature that when studying the dynamic characteristics of the motorized spindle system, some research has studied the thermal effect during the operation of the motorized spindle system. In addition, when calculating the total stiffness matrix of the motorized spindle system, the bearing contact stiffness is considered, while the influence of the film stiffness on the bearing is ignored. In this paper, the comprehensive stiffness model of the angular contact ball bearing of the motorized spindle system is established when the high-speed effect and the thermal effect are coupled. Based on the comprehensive stiffness, according to the structure of the motorized spindle unit and Timoshenko beam theory, the dynamic model of the motorized spindle system is established using the finite element method. The effects of different working conditions on the dynamic characteristics of the spindle system, such as natural frequency and critical speed, are investigated.

2 Calculation method of comprehensive stiffness of ACBB

2.1 Contact stiffness model of ACBB

To ensure the rationality of the modeling, the following assumptions are made:

1. The influence of the cage on the static balance of bearing is ignored, and the bearing is only subject to axial force.
2. The motion of the rolling element on the raceway is pure rolling.
3. The contact between the rolling body and the inner and outer raceways is the Hertz contact.
4. During high-speed operation, the interaction force between the cage and the rolling elements is very limited, so the role of the cage is ignored in the force analysis of the bearing.

The ACBB generates friction due to the contact of various parts during operation, which will cause friction heat generation. The higher the rotation speed, the more heat will be generated. The internal temperature of the bearing will gradually increase through heat conduction and heat convection, resulting in the thermal expansion of various parts of the bearing. When calculating the thermal deformation of the bearing inner ring, outer ring and rolling element, the calculation method proposed by Harris (1971) is generally adopted:

$$\begin{cases} u_{\mathrm{i}} = \alpha_{\mathrm{i}} d_{\mathrm{i}} \Delta T_{\mathrm{i}} \\ u_{\mathrm{b}} = \alpha_{\mathrm{b}} d_{\mathrm{b}} \Delta T_{\mathrm{b}} \\ u_{\mathrm{o}} = \alpha_{\mathrm{o}} d_{\mathrm{o}} \Delta T_{\mathrm{o}}, \end{cases} \tag{1}$$

where u_{i}, u_{o} and u_{b} are the thermal deformation of the inner ring, outer ring and rolling element, respectively; and α_{i}, α_{o} and α_{b} are the thermal expansion coefficient of the inner ring, outer ring and rolling element materials, respectively. ΔT_{i}, ΔT_{o} and ΔT_{b} are the inner ring, outer ring and rolling temperature rise, respectively; and d_{i}, d_{o} and d_{b} are the diameters of the inner ring, outer ring and rolling element, respectively.

According to Eq. (1), the sum of the radial and axial thermal deformation δ_{r} and δ_{a} of the ACBB assembled face to face during high-speed operation due to temperature rise is respectively

$$\begin{cases} \delta_{\mathrm{r}} = u_{\mathrm{i}} - 2u_{\mathrm{b}} - u_{\mathrm{o}} \\ \delta_{\mathrm{a}} = \frac{\alpha_h L_h \Delta T_h - \alpha_s L_s \Delta T_s}{2}. \end{cases} \tag{2}$$

When the bearing runs at high speed, the inner and outer rings and rolling elements of the bearing are subjected to centrifugal force, resulting in radial centrifugal deformation. Due to the bearing assembly, the bearing outer ring is installed in the bearing seat hole. Since the deformation of the bearing outer ring is small, the centrifugal deformation of the outer ring is ignored. The radial deformation of the inner ring due to the centrifugal effect δ_1 is (Li et al., 2020)

$$\delta_1 = \frac{\rho_{\mathrm{i}} \omega^2}{16 E_{\mathrm{i}}} \left[(3 + \nu_{\mathrm{i}}) D_{\mathrm{i}}^2 + (1 - \nu_{\mathrm{i}}) d_{\mathrm{i}}^2 \right] D_{\mathrm{i}}, \tag{3}$$

where ρ_{i} is the material density of the bearing inner ring, E_{i} is the elastic modulus of the bearing inner ring material, D_{i}

is the inner channel diameter and ν_i is the Poisson's ratio of the bearing inner ring material.

Considering the thermal deformation and centrifugal deformation of the ACBB, a modified quasi-static bearing model has been established. The contact stiffness of the ball bearing could then be obtained according to the relationship between the contact load and the contact deformation (Du et al., 2001).

$$K_{cj} = \frac{\mathrm{d}Q_j}{\mathrm{d}\delta_j} = 1.5\Gamma_j^{-1}\left[\left(\frac{9}{2\varepsilon_j \Sigma\rho_j}\right)\left(\frac{1}{\pi\kappa_j E}\right)^2\right]^{-1/3} Q_j^{1/3}, \quad (4)$$

where K_{cj} is the contact stiffness of the ball bearing; Q_j is the contact load of two contact objects; δ_j is the contact deformation of two contact objects; Γ and ε are complete elliptic integrals of the first and second kinds, respectively; and κ is an elliptic rate parameter.

$$\Gamma = \int_0^{\frac{\pi}{2}} \left[1 - \left(1 - \frac{1}{\kappa^2}\right)\sin^2\varphi\right]^{-\frac{1}{2}} \mathrm{d}\varphi \quad (5)$$

$$\varepsilon = \int_0^{\frac{\pi}{2}} \left[1 - \left(1 - \frac{1}{\kappa^2}\right)\sin^2\varphi\right]^{\frac{1}{2}} \mathrm{d}\varphi \quad (6)$$

2.2 Film stiffness model of ACBB considering spinning and temperature

According to the motion form and characteristics of the spin motion of the ACBB, the motion form is equivalent to the motion of an ellipsoid on an infinite plane at the average speed u_b of the rolling element and raceway (Liu et al., 2023). Meanwhile, the plane rotates at the spin angular velocity ω_s. The velocity components at any point in the contact area are v_R and u_R, respectively. When the rolling element contacts the inner and outer raceways, the comprehensive elastic modulus is E, the equivalent radius of curvature is R_a and β is the attitude angle of bearing.

$$E = 2/\left(\frac{1-\nu_1^2}{E_1} + \frac{1-\nu_2^2}{E_2}\right) \quad (7)$$

$$R_a = \frac{R_1 R_2}{R_1 \pm R_2} \quad (8)$$

$$\begin{cases} u_R(x,y) = \frac{\omega_s y}{2} + u_b \\ v_R(x,y) = -\frac{\omega_s x}{2} \end{cases} \quad (9)$$

$$u_b = D_b\omega_r(\sin\beta\sin\alpha_{ij} + \cos\beta\cos\alpha_{ij})/2 \quad (10)$$

$$\beta = \arctan(\sin\alpha_0/(\cos\alpha_0 + \gamma)), \quad (11)$$

where, according to the inner and outer rings of the bearing, ω_s is divided into ω_{si} and ω_{so}. The calculation formulas are as follows:

$$\begin{cases} \omega_{si} = \omega_r\sin(\alpha_{ij} - \beta) - (\omega_i - \omega_m)\sin\alpha_{ij} \\ \omega_{so} = \omega_m\sin\alpha_{oj} - \omega_r\sin(\alpha_{oj} - \beta), \end{cases} \quad (12)$$

where $\gamma = \frac{D_b}{d_m}$; d_m is the pitch diameter of the ACBB; and E_1, E_2, v_1, v_2, R_1 and R_2 are the elastic modulus, Poisson's ratio and radius of curvature of the two contacts, respectively. Among them, "+" is the external contact and "−" the internal contact. ω_{si} and ω_{so} are the spinning angular speed of the bearing inner ring and outer ring, respectively; α_{ij} and α_{oj} are the contact angle of the inner and outer rings, respectively; ω_m is the orbital speed of the ball; ω_i is the inner ring angular speed of the bearing; and ω_r is the speed of the ball about its own axis. The calculation formulas are as follows:

$$\omega_r = \frac{-\omega_s}{\left(\frac{\cos\alpha_{oj}+\tan\beta\sin\alpha_{oj}}{1+\frac{D_b}{d_m}\cos\alpha_{oj}} + \frac{\cos\alpha_{ij}+\tan\beta\sin\alpha_{ij}}{1-\frac{D_b}{d_m}\cos\alpha_{ij}}\right)\left(\frac{D_b}{d_m}\right)\cos\beta} \quad (13)$$

$$\omega_m = \frac{1 - \left(\frac{D_b}{d_m}\right)\cos\alpha_{ij}}{1 + \cos\left(\alpha_{ij} - \alpha_{oj}\right)}\omega_s. \quad (14)$$

Considering the influence of spin motion, the Reynolds equation of point contact lubrication is described as follows:

$$\frac{\partial}{\partial x}\left(\frac{\rho h^3}{\eta}\frac{\partial p}{\partial x}\right) + \frac{\partial}{\partial y}\left(\frac{\rho h^3}{\eta}\frac{\partial p}{\partial y}\right) = 12\frac{\partial}{\partial x}(u_R\rho h) + 12\frac{\partial}{\partial x}(v_R\rho h). \quad (15)$$

The boundary conditions are expressed by

$$\begin{cases} P(X_0, Y) = 0 \\ P(X_e, Y) = 0, \frac{\partial P(X_e, Y)}{\partial X} = 0 \\ P|Y = \pm 1 = 0. \end{cases}$$

Considering the influence of temperature on lubricant viscosity, the viscosity pressure formula by Roelands (1966) and Wen and Yang (1992) is adopted.

$$\eta = \eta_0 \exp\left\{(\ln\eta_0 + 9.67)\left[(1 + p/p_0)^z\left(\frac{T-138}{T_0-138}\right)^{-1.1} - 1\right]\right\}, \quad (16)$$

where η_0 is the dynamic viscosity of lubricating under normal pressure, p is the pressure, p_0 is the pressure coefficient and z is the viscous pressure coefficient.

The density-pressure-temperature equation of bearing under elastohydrodynamic lubrication (EHL) is shown in Eq. (17):

$$\rho = \rho_0\left(1 + \frac{0.6p}{1+1.7p} + D(T - T_0)\right), \quad (17)$$

where ρ is the density of lubricating oil, P is the pressure and ρ_0 is the density of lubricating oil under atmospheric pressure.

When the lubricating oil flows between the rolling element and the inner and outer ring, it will be affected by the contact load, and its balance equation is expressed by

$$w = \int_{x_0}^{x_e}\int_{y_0}^{y_e} p\,\mathrm{d}x\,\mathrm{d}y. \quad (18)$$

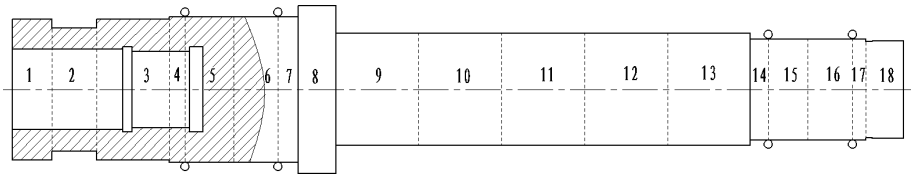

Figure 1. Finite element partition diagram of the rotor-bearing system.

Table 1. Bearing parameters.

Name	Value
Bearing internal diameter D_i/mm	65
Bearing external diameter D_o/mm	100
Rolling element diameter D_d/mm	8.73
Number of rolling elements	25
Bearing width B/mm	18
Initial contact angle α^0/°	15
Rolling element density/g cm^{-3}	3.2
Inner groove curvature coefficient f_i/mm	0.56
Outer groove curvature coefficient f_o/mm	0.53

Table 2. Comparison of calculated results and test results.

	Test result	Calculation results
f (Hz)	537.1	589.81
n (r/min)	32226	35388
Error	–	9.81 %

According to the definition of stiffness, the basic formula for bearing film stiffness is shown in Eq. (19):

$$K_{\text{film}} = \lim_{\delta \to 0} \frac{\Delta w}{\delta} = -\frac{\mathrm{d}w}{\mathrm{d}h_{\min}}. \tag{19}$$

According to Formulas (15)–(18) and the minimum oil film thickness $h_{\min}$ formula (Gupta, 1979), considering spin and temperature, it can be derived that

$$K_{\text{film}} = -\frac{\mathrm{d}w_{\text{film}}}{\mathrm{d}h_{\min}} = 13.6986 \left[\frac{R_x}{3.63U^{0.68}G^{0.49}\left(1-e^{-0.68k}\right)} \right] \times ER_x^2 \left[\frac{h_{\min}R_x}{3.63U^{0.68}G^{0.49}\left(1-e^{-0.68k}\right)} \right]^{-14.6986} \tag{20}$$

$$K_{\text{films}} = -\frac{\mathrm{d}w_{\text{films}}}{\mathrm{d}h_{\text{mins}}} = 0.16219ER_x^3 / \left[0.1077 \times 10^3 R_x h_{\text{mins}} - 0.9588G^{0.8001} \times U^{0.72}k^{1.616}\left(1+21.459e^{-0.3k}\right) \times \left(1-1.3101 \times 10^{10}\Omega_s^{1.024}\right) \right]. \tag{21}$$

In the formula, U is the velocity parameter, G is the material parameter, k is ellipticity, Ω_s is spinning velocity parameter, K_{film} is the oil film stiffness without considering spin motion and K_{films} is the oil film stiffness when considering spin motion and temperature rise. The range of values for each parameter in the above equation can be found in Li et al. (2020).

2.3 Comprehensive stiffness model of ACBB

The contact stiffness and film stiffness of the ACBB are combined in series to establish the comprehensive stiffness model in this paper. The comprehensive stiffness between the jth rolling element and the inner and outer rings is as follows:

$$\frac{1}{K_{qij}} = \frac{1}{K_{\text{ci}j}} + \frac{1}{(K_{\text{oil}})_{ij}} \tag{22}$$

$$\frac{1}{K_{qoj}} = \frac{1}{K_{\text{co}j}} + \frac{1}{(K_{\text{oil}})_{oj}}, \tag{23}$$

where $(K_{\text{oil}})_{ij}$ and $(K_{\text{oil}})_{oj}$ are the film stiffness between the jth rolling element and the inner ring and outer ring, respectively; and $K_{\text{ci}j}$ and $K_{\text{co}j}$ are the contact stiffness between the jth rolling element and the inner and outer ring, respectively.

According to the calculation formula of bearing comprehensive stiffness, the comprehensive stiffness components $K_{\text{ri}j}$ and $K_{\text{ai}j}$ of the jth rolling element and inner ring in the radial and axial direction, and the comprehensive stiffness components $K_{\text{ro}j}$ and $K_{\text{ao}j}$ of the outer ring in the radial and axial direction, are as follows:

$$K_{\text{ri}j} = K_{qij}\cos^2\alpha_{ij} \tag{24}$$

$$K_{\text{ai}j} = K_{qij}\sin^2\alpha_{ij} \tag{25}$$

$$K_{\text{ro}j} = K_{qoj}\cos^2\alpha_{oj} \tag{26}$$

$$K_{\text{ao}j} = K_{qoj}\sin^2\alpha_{oj}. \tag{27}$$

For the ACBB, the entire comprehensive stiffness can be derived from the stiffness between the rolling element and

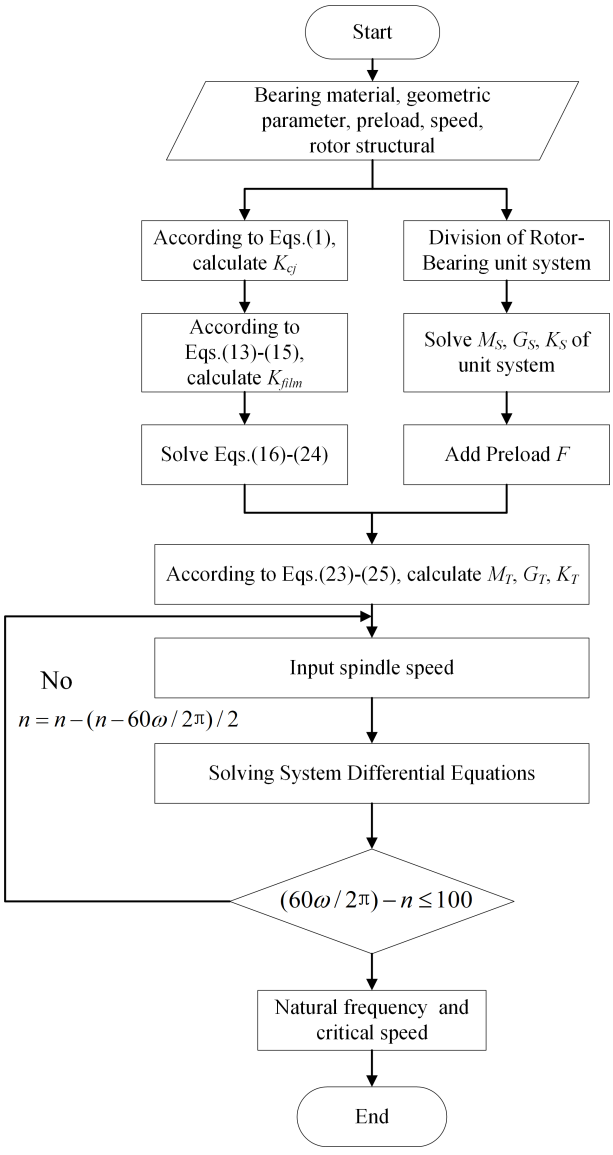

Figure 2. Calculation flowchart.

the inner ring and outer ring:

$$K_{\mathrm{a}} = \sum_{j=1}^{j=Z} \frac{K_{\mathrm{a}ij} K_{\mathrm{a}oj}}{K_{\mathrm{a}ij} + K_{\mathrm{a}oj}} \tag{28}$$

$$K_{\mathrm{r}} = \sum_{j=1}^{j=Z} \frac{K_{\mathrm{r}ij} K_{\mathrm{r}oj}}{K_{\mathrm{r}ij} + K_{\mathrm{r}oj}} \cos^2\left[\frac{2\pi}{Z}(j-1)\right] \tag{29}$$

$$K_{\theta} = \frac{d_m^2}{4} \sum_{j=1}^{j=Z} \frac{K_{\mathrm{a}ij} K_{\mathrm{a}oj}}{K_{\mathrm{a}ij} + K_{\mathrm{a}oj}} \cos^2\left[\frac{2\pi}{Z}(j-1)\right], \tag{30}$$

where K_{a}, K_{r} and K_{θ} are the comprehensive axial stiffness, comprehensive radial stiffness and comprehensive angular stiffness of the ACBB, respectively.

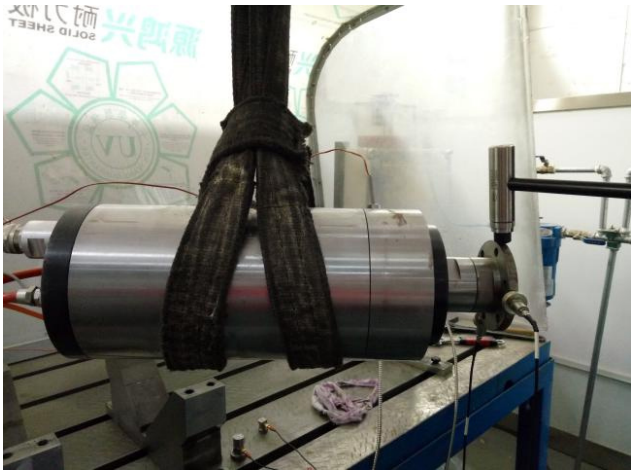

Figure 3. Schematic diagram of static hammering.

3 Dynamic model of motorized spindle system

In order to study the dynamical characteristics of the motorized spindle system, the dynamical mathematical model of the system should first be established. In this paper, the dynamic model of the motorized spindle system is established by using the finite element method. The spindle unit is discretized, and each element is regarded as a Timoshenko beam element, which considers the shear effect. Figure 1 is the finite element partition diagram of the rotor-bearing system. The rotor is divided into 18 elements and 19 nodes, and each node has 4 degrees of freedom. Among them, nodes 5, 7, 15 and 17 are the location of the support bearing.

According to the structure and function characteristics of the motorized spindle, the motion equation of the motorized spindle system is established. Since the damping value of the motorized spindle is relatively small, its influence on the dynamics of the system is ignored, and the effect of the gyroscopic moment will cause the movement trajectory of the spindle to deviate from the central axis. Therefore, it is necessary to consider the influence of the gyroscopic matrix of the axis unit and additional unit on the system, and the system motion equation is

$$M_{\mathrm{T}}\ddot{x} + \Omega G_{\mathrm{T}}\dot{x} + K_{\mathrm{T}}x = F, \tag{31}$$

where M_{T}, G_{T}, K_{T} and F are the total mass matrix, total gyroscopic matrix, total stiffness matrix and total load column vector of the system, respectively.

$$M_{\mathrm{T}} = M_{\mathrm{t}} + M_{\mathrm{R}} + M_d \tag{32}$$

$$K_{\mathrm{T}} = K_{\mathrm{S}} + K_{\mathrm{b}}, \tag{33}$$

where M_{t} and M_{R} represent the translational and rotational mass matrix of the spindle, respectively; M_d is the equivalent mass matrix of the additional parts; and K_{S} and K_{b} are the stiffness matrix of the spindle and the angular contact ball

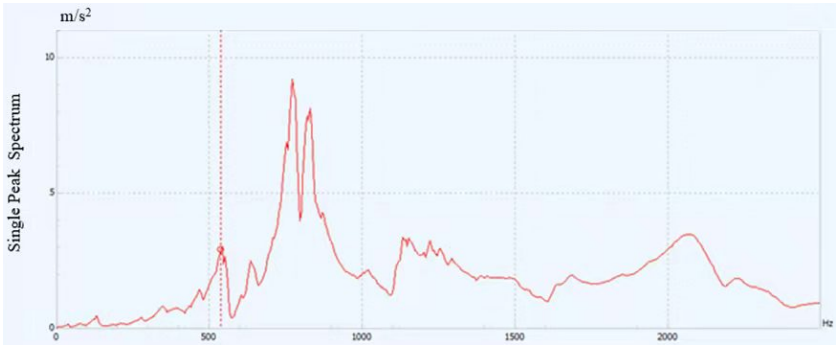

Figure 4. Response spectrum of the modal test.

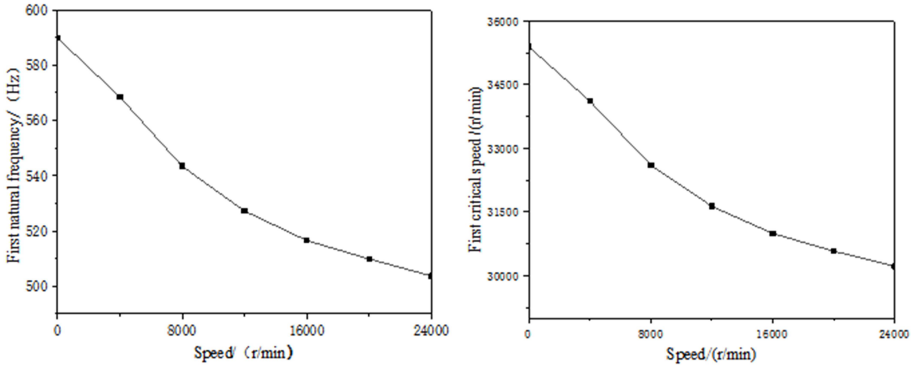

Figure 5. Effect of rotational speed on natural frequency and critical speed of the system.

bearing, respectively. In this paper, the comprehensive stiffness matrix of the ball bearing is adopted to calculate the total stiffness matrix of the system.

The steps to solve the dynamic model of the motorized spindle system are as follows: first, the spindle is discretized, and each element divided is regarded as a Timoshenko beam element. Then, the mass matrix, stiffness matrix, gyroscope matrix and load and displacement column vectors of each element are determined, and the total mass matrix, stiffness matrix, gyroscope matrix, total load and displacement column vectors of the system are superimposed and combined according to the method of matching. Finally, the dynamic parameters of the motorized spindle system are obtained by solving the differential equations of the system. After considering the comprehensive stiffness of the ACBB, the solution process for its overall dynamic characteristics is shown in Fig. 2, and the performance parameters of the bearing are shown in Table 1.

4 Test verification

The dynamic characteristics of the motorized spindle system are measured by the static hammering method, as shown in Fig. 3. During measurement, the motorized spindle is in a free state, and the exciting force is applied on the spindle end by the force hammer. The excitation signal of the force sensor and the response signal measured by the acceleration sensor are transmitted to the computer, and the frequency response of the motorized spindle system is obtained by the analysis software, as shown in Fig. 4.

It can be seen from Fig. 4 that the first peak appears at 537.1 Hz, which could be judged as the first natural frequency of the system. The first critical speed can be calculated according to the formula $n = 60f$. Table 1 shows the comparison between the calculated results and the experimental results.

There is a certain error between the test results and the calculation results in Table 2. This is because some structures of the spindle have been simplified in the process of establishing the dynamic model. However, the margin of error is within 10 %, which is relatively small. This shows the validity and reliability of the finite element dynamic model of the motorized spindle system established in this paper.

5 Dynamic characteristics analysis of motorized spindle based on comprehensive stiffness of ACBB

At high speed, the mechanical properties of the ACBB have an obvious influence on the dynamic characteristics of the

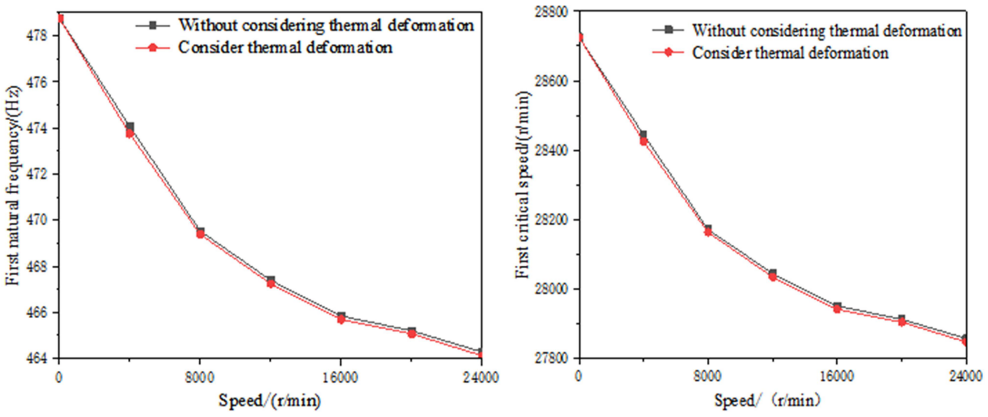

Figure 6. Effect of thermal deformation on natural frequency and critical speed of the system.

motorized spindle system. The change of preload, axial external load and lubrication performance of the ACBB will greatly influence the comprehensive stiffness of the ACBB and then further affect the performance of the whole motorized spindle system. The influence of different factors such as bearing preload, bearing thermal deformation, external load and spindle speed on the dynamic characteristics of the motorized spindle system is studied in this paper, which considers the high-speed effect and thermal effect.

5.1 Effect of speed

When the ACBB preload Fa = 500 N, the natural frequency and critical speed of the motorized spindle system at different ACBB speeds are given in Fig. 5. With the increase in the speed of the motorized spindle, the natural frequency and critical speed of the system show a downward trend. This is because the contact stiffness and film stiffness are in the same order of magnitude and decrease, and the comprehensive stiffness of the ACBB decreases under the action of the series, which results in a downward trend in the natural frequency and critical speed of the system.

5.2 Effect of the thermal deformation of ACBB

When the motorized spindle rotates at high speed, the friction of the ACBB leads to an increase in the temperature and heat generation in the internal parts. This causes the thermal deformation of the ACBB and affects the dynamic characteristics of the system. Figure 6 shows the variation of the natural frequency and critical speed of the system when considering the thermal deformation of the ACBB at different speeds. It can be seen from Fig. 6 that the natural frequency and critical speed of the system are reduced when considering thermal deformation. This shows that the influence of thermal deformation on the dynamic characteristics of the ACBB should be considered when establishing a dynamic model of ball bearings, and the thermal deformation of the ACBB should be reduced as much as possible.

5.3 Effect of the preload of ACBB

As shown in Fig. 7, the natural frequency and critical speed of the system increase with increasing preload. The reason for this phenomenon is that the comprehensive stiffness of the bearing increases, and the total stiffness of the system increases with the increase in bearing preload. The increase in initial preload of the ACBB could improve the stability of the system, but the preload cannot be too large, which will reduce the service life of the bearing.

5.4 Effect of external load

When a constant axial external load is applied to the motorized spindle system, it will cause a change in the comprehensive stiffness of the supporting ACBB, thus affecting the dynamic performance of the system. As shown in Fig. 8, the natural frequency and critical speed of the system increase with the increase in the axial external load. The reason for this phenomenon is that the increase in the axial external load results in an increase in the comprehensive stiffness of the bearing, therefore the natural frequency and critical speed of the system increase. At the same time, with the increase in the speed of the motorized spindle, the natural frequency and critical speed of the system first decrease and then increase. This is because the speed increases, and the dynamic viscosity of the lubricating oil of the ACBB decreases due to the influence of temperature rise. The film stiffness then increases, which results in an increase in the comprehensive stiffness of the ACBB. Therefore, there is an inflection point in the figure.

6 Conclusions

In this paper, according to the characteristics of a high-speed motorized spindle, the comprehensive stiffness model of its support bearing is first established. On this basis, a dynamic model of a motorized spindle system is proposed using Timoshenko beam element theory and the finite element method.

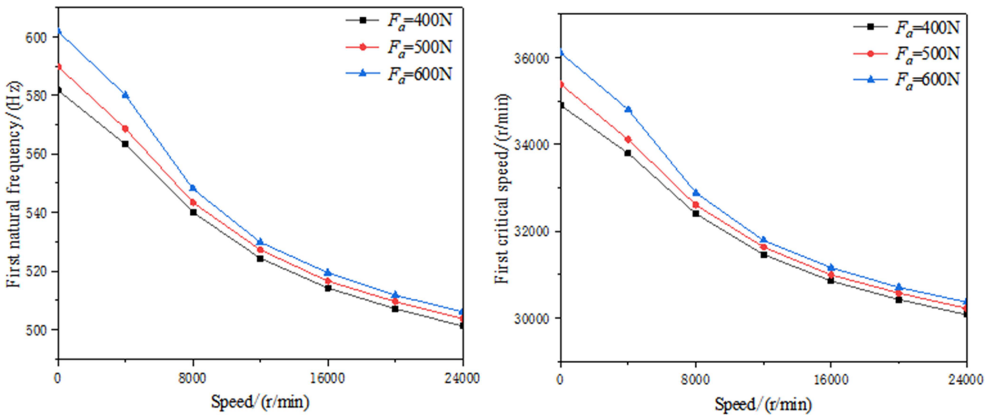

Figure 7. Effect of preload on natural frequency and critical speed of the system.

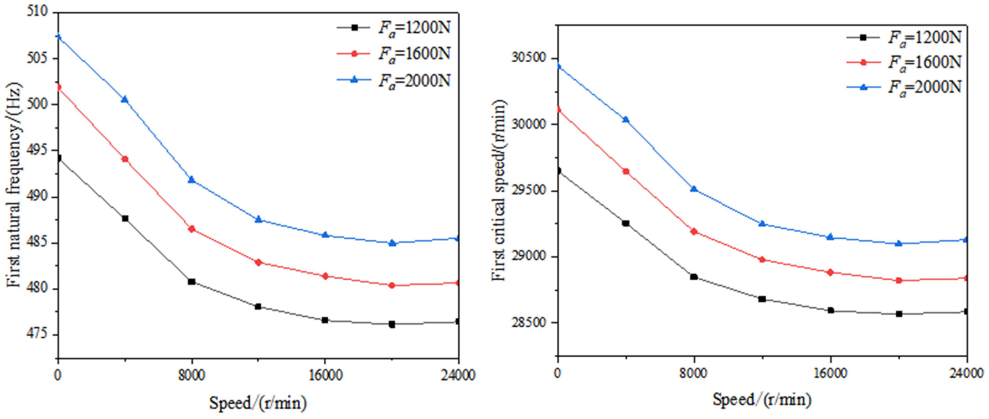

Figure 8. Effect of external load on natural frequency and critical speed of the system.

Subsequently, the dynamic characteristics of the high-speed motorized spindle system under the combined action of the high-speed effect and thermal effect are solved and verified by experiments. Finally, the influence of operating speed, thermal deformation of the ACBB, and preload and external load on the dynamic characteristics of the spindle system are studied. The following conclusions are obtained:

1. At high speed, the change of comprehensive stiffness of the ACBB directly affects the overall stiffness of the system and then influences the dynamic characteristics of the system, such as natural frequency and critical speed.

2. With the increase in motorized spindle speed, the comprehensive stiffness of the ACBB decreases, which leads to a decrease in the natural frequency and critical speed. At the same time, the ACBB will produce the thermal deformation during operation, which will reduce the natural frequency and critical speed of the system.

3. The increase in the ACBB preload increases the comprehensive stiffness of the ACBB, increases the natural frequency and critical speed of the motorized spindle system and effectively improves the stability of the system.

4. The axial external load acting on the motorized spindle system changes the comprehensive stiffness of the ACBB and changes the natural frequency and critical speed of the system.

Data availability. The data that support the findings of this study are available from the corresponding author upon reasonable request.

Author contributions. All authors contributed to the research on the dynamic characteristics of the motorized spindle based on the comprehensive stiffness of the angular contact ball bearing. DBQ wrote the paper and conducted experiments. LCL conducted overall algorithm validation and revised the paper. LK conducted graphic and textual drawing and handled the paper submission. SRZ established and calculated the dynamic model. CP conducted the vibration model design and analysis.

Competing interests. The contact author has declared that none of the authors has any competing interests.

Disclaimer. Publisher's note: Copernicus Publications remains neutral with regard to jurisdictional claims made in the text, published maps, institutional affiliations, or any other geographical representation in this paper. While Copernicus Publications makes every effort to include appropriate place names, the final responsibility lies with the authors. Views expressed in the text are those of the authors and do not necessarily reflect the views of the publisher.

Acknowledgements. This work was financially supported by the National Natural Science Foundation of China (grant no. 51465035) and the Natural Science Foundation of Gansu Province of China (grant no. 20JR5RA466).

Financial support. This research has been supported by the Innovative Research Group Project of the National Natural Science Foundation of China (grant nos. 51465035) and the Natural Science Foundation of Gansu Province of China (grant no. 20JR5RA466).

Review statement. This paper was edited by Fulei Ma and reviewed by two anonymous referees.

References

Cao, H. R., Li, B., and He, Z. J.: Dynamic modeling of high-speed spindles and analysis of high-speed effects, Journal of Vibration Engineering, 25, 2, 103–109, 2012.

Cao, Y. Z. and Yusuf, A.: A general method for the modeling of spindle-bearing systems, Journal of Mechanical Design, 126, 6, 1089–1104, 2004.

Chen, B., Chen, J., and Dong, M. L.: Modeling method analysis for oil film stiffness calculation based on point contact TEHL theory, Lubrication Engineering., 38, 70–75, 2013.

Cheng, Y. W.: Thermal mechanical dynamic characteristic research of high speed motorized spindle, MS, Lanzhou University of Technology, Lanzhou, 30–50, 2019 (in Chinese).

Du, Y. H., Qiu, M., and Jiang, X. Q.: Stiffness Calculation of High Speed Precision Angular Contact Ball Bearing, Bearing, 11, 5–8+43, 2001.

Fang, B., Yan, K., and Hongetal, J.: A comprehensive study on the off-diagonal coupling elements in the stiffness matrix of the angular contact ball bearing and their influence on the dynamic characteristics of the rotor system, Mechanism and Machine Theory, 158, https://doi.org/10.1016/j.mechmachtheory.2021.104251, 2021.

Fawzi, M. A.: Finite element modeling of a rotor shaft rolling bearings system with consideration of bearing nonlinearities, Journal of Vibration and Control, 4, https://doi.org/10.1177/107754639800400503, 1998.

Gupta, P. K.: Dynamics of rolling-element bearings-part I: cylindrical roller bearing analysis, J. Tribol., 101, 293, https://doi.org/10.1115/1.3453357, 1979.

Harris, T. A. : An Analytical Method to Predict Skidding in Thrust-Loaded, Angula-Contact Ball Bearings, Journal of Lubrication Technology, 93, 17–23, https://doi.org/10.1115/1.3451511, 1971.

Holkup, T. Y. and Cao, H. R.: A comparative study on the dynamics of high speed spindles with respect to different preload mechanisms, International Journal of Advanced Manufacturing Technology, 57, 871–883, 2011.

Jorgensen, B. R. and Shin, Y. C.: Dynamics of spindle-bearing systems at high speeds including cutting load effects, Journal of Manufacturing Science and Engineering, 120, 387–394, 1998.

Lei, C. L., Cui, P., and Cao, P. Y.: Research on comprehensive stiffness characteristics of angular contact ball bearings under multi-factor coupling condition, Journal of Advanced Mechanical Design, Systems, and Manufacturing, 15, 1–18, 2021.

Lei, C. L., Li, F. H., and Gong, B. R.: An integrated model to characterize comprehensive stiffness of angular contact ball bearings, Mathematical Problems in Engineering, 4, 1–12, 2020.

Li, J. H., Lei, C. L., and Gong, B. R.: Modeling and analysis of the composite stiffness for angular contact ball bearings, Shock and Vibration, https://doi.org/10.1155/2020/8832750, 2020.

Li, S. S.: Study on Dynamic characteristics of ball bearing-rotor system in ultra high speed spindles, MS, Shanghai University, 40–56, 2006 (in Chinese).

Li, Y., Wu, K., Wang, N., Wang, Z., Li, W. Q., and Lei, M. H.: Thermal deformation analysis of motorized spindle base on thermo-solid structure coupling theory, Heat Mass Transfer, 60, 1755–1771, 2024.

Li, Z., Guan, X. L., and Zhong, Y.: Analysis of dynamic characteristics of angle contact bearings with combined loads, Journal of Mechanical Engineering., 56, 116–125, 2020.

Liu, K., Lei, C. L., Song, R. Z., and Wei, X.: Study on friction characteristics of angular contact ball bearing with local defects, Journal of Advanced Mechanical Design, Systems, and Manufacturing, 17, 1–18, 2023.

Lin, C. W., Tu, J. F., and Kamman, J.: An integrated thermal-machanical dynamic model to characterize motorized machine tool spindles during very high speed rotation, International Journal of Machine Tools & Manufacture., 43, 1035–1050, 2003.

Nelson, H. D.: A finite rotating shaft element using Timoshenko beam theory, Journal of Mechanical Design, 102, 793–803, 1980.

Noel, D., Ritou, M., and Furetet, B.: Complete analytical expression of the stiffness matrix of angular contact ball bearings, Journal of Tribology, 135, 1–8, 2013.

Roelands, C. J. A.: Correlational aspects of the viscosity-temperature-pressure relationship of Lubricating oils, Durk, U R B, Groningen, https://doi.org/10.1115/1.3451519, 1966.

Wang, Z., Chen, S., Wang, Z., Niu, S. Q., and Hu, B. B.: Nonlinear dynamic characteristics of ceramic motorized spindle considering unbalanced magnetic pull and contact force effects, J. Braz. Soc. Mech. Sci. Eng., 46, 119, https://doi.org/10.1007/s40430-024-04692-6, 2024.

Wen, S. Z. and Yang, P. R.: Elastohydrodynamic lubrication, Tsinghua University Press, ISBN 9787302010000, 1992.

Wu, H.: Research on the dynamic characteristics of rolling element bearings and the dynamic model of bearing rotor system, MS, East China University of Science and Technology, 22–31, 2011 (in Chinese).

Zhang, P. and Chen, X. A.: Thermal-mechanical coupling model-based dynamical proper tie analysis of a motorized spindle system, Proc. IMechE Part B: J. Engineer. Manufacture, 230, 4, 732–743, 2016.